



HAL
open science

Towards safe phosphine oxides photoinitiators with good cytocompatibility for 3D printing of thermoplastics

Loïc Buchon, Jean-michel Becht, Laurent Rubatat, Wei Wang, Hua Wei, Pu Xiao, Jacques Lalevee

► To cite this version:

Loïc Buchon, Jean-michel Becht, Laurent Rubatat, Wei Wang, Hua Wei, et al.. Towards safe phosphine oxides photoinitiators with good cytocompatibility for 3D printing of thermoplastics. *Journal of Applied Polymer Science*, 2023, 10.1002/app.54694 . hal-04224400

HAL Id: hal-04224400


<https://univ-pau.hal.science/hal-04224400>

Submitted on 2 Oct 2023

HAL is a multi-disciplinary open access archive for the deposit and dissemination of scientific research documents, whether they are published or not. The documents may come from teaching and research institutions in France or abroad, or from public or private research centers.

L'archive ouverte pluridisciplinaire **HAL**, est destinée au dépôt et à la diffusion de documents scientifiques de niveau recherche, publiés ou non, émanant des établissements d'enseignement et de recherche français ou étrangers, des laboratoires publics ou privés.

Towards safe phosphine oxides photoinitiators with good cytocompatibility for 3D printing of thermoplastics

Loïc Buchon^{1,2} | Jean-Michel Becht^{1,2} | Laurent Rubatat³ | Wei Wang⁴ |
Hua Wei⁴ | Pu Xiao⁵ | Jacques Lalevee^{1,2} 

¹Université de Haute-Alsace, CNRS, IS2M UMR 7361, Mulhouse, France

²Université de Strasbourg, Strasbourg, France

³Université de Pau et des Pays de l'Adour, E2S UPPA, CNRS, IPREM, Pau, France

⁴Hunan Province Cooperative Innovation Center for Molecular Target New Drug Study & School of Pharmaceutical Science, University of South China, Hengyang, China

⁵Research School of Chemistry, Australian National University, Canberra ACT, Australia

Correspondence

Jacques Lalevee, Université de Haute-Alsace, CNRS, IS2M UMR 7361, F-68057 Mulhouse, France.

Email: jacques.lalevee@uha.fr

Funding information

agence nationale de la recherche, Grant/Award Number: ANR-19-CE06-0017

Abstract

3D printing is the technology of choice for the rapid production of objects with complex morphologies and controlled physical and chemical properties. 3D printing by photopolymerization is of great interest because of its ability to access very small scales and its high resolution. In the case of recent 3D printers, the preferred wavelength for light irradiation is 405 nm since it is a safe and energy-economical irradiation. For 3D printing to be effective, it is therefore necessary to develop easily accessible, stable and highly efficient photoinitiating systems at the 405 nm wavelength. Beside, with the increasing use of photoinitiators, it is essential to develop structures with low cytotoxicity. Hence, the development of new photoinitiators is currently of major interest. To this end, the photochemical properties (triplet energy, bond dissociation energy, cleavage reaction enthalpy, and absorption properties) of several molecules have been calculated by molecular modeling and the most promising compounds have been synthesized. In this paper, four phosphine oxides photoinitiators (ADPO-1, CPO-2, CPO-3, and FPO-1) are synthesized and characterized. Subsequently, their absorption properties are measured and their efficiencies in photopolymerization under LED irradiation at 405 nm are evaluated. It is important to note that these structures have never been reported in 3D printing. Markedly, among the obtained photoinitiators, two of them show better efficiency than the commercially available and widely used phenylbis(2,4,6-trimethylbenzoyl)phosphine oxide (BAPO) in photopolymerization (i.e., $(Rp/[M_0]) \times 100$ values are 6.94, 12.95, and 4.93 s^{-1} for CPO-2, ADPO-1, and BAPO; with $[M_0]$ the initial acrylate function concentration). Furthermore, one of the synthesized photoinitiators is successfully used in 3D printing of thermoplastics for potential recycling ability. Finally, one of the obtained structures shows a lower cytotoxicity than the benchmark structure diphenyl(2,4,6-trimethylbenzoyl)phosphine oxide (TPO).

KEYWORDS

photochemistry, photopolymerization, radical polymerization

This is an open access article under the terms of the [Creative Commons Attribution](https://creativecommons.org/licenses/by/4.0/) License, which permits use, distribution and reproduction in any medium, provided the original work is properly cited.

© 2023 The Authors. *Journal of Applied Polymer Science* published by Wiley Periodicals LLC.

1 | INTRODUCTION

In recent years, 3D printing, also known as additive manufacturing, has experienced significant development.¹ This technology, combined with computer-assisted design (CAD), allows the rapid production of objects with complex morphologies² and controlled physical/chemical properties.³ Therefore, flexible materials,⁴ shape memory,⁵ or controlled porosity⁶ materials are easily accessible. There are multiple methods of 3D printing such as fused deposition modeling, powder bed fusion, and vat photopolymerization.⁷ The last method has better accuracy than other technologies and often gives access to smaller scales.^{5,8} In 3D printing by vat photopolymerization, three types of technologies are commonly used, that is, stereolithography (SLA) where a laser irradiates the resin dot by dot, digital light processing (DLP) where the irradiation of the resin is done layer by layer with a projector, and liquid crystal display (LCD) where a screen is used to polymerized the resin layer by layer.^{9,10} Although the SLA method is more accurate than DLP and LCD, the latter ones are becoming increasingly popular as they allows significantly shorter printing time at lower cost.^{9–11}

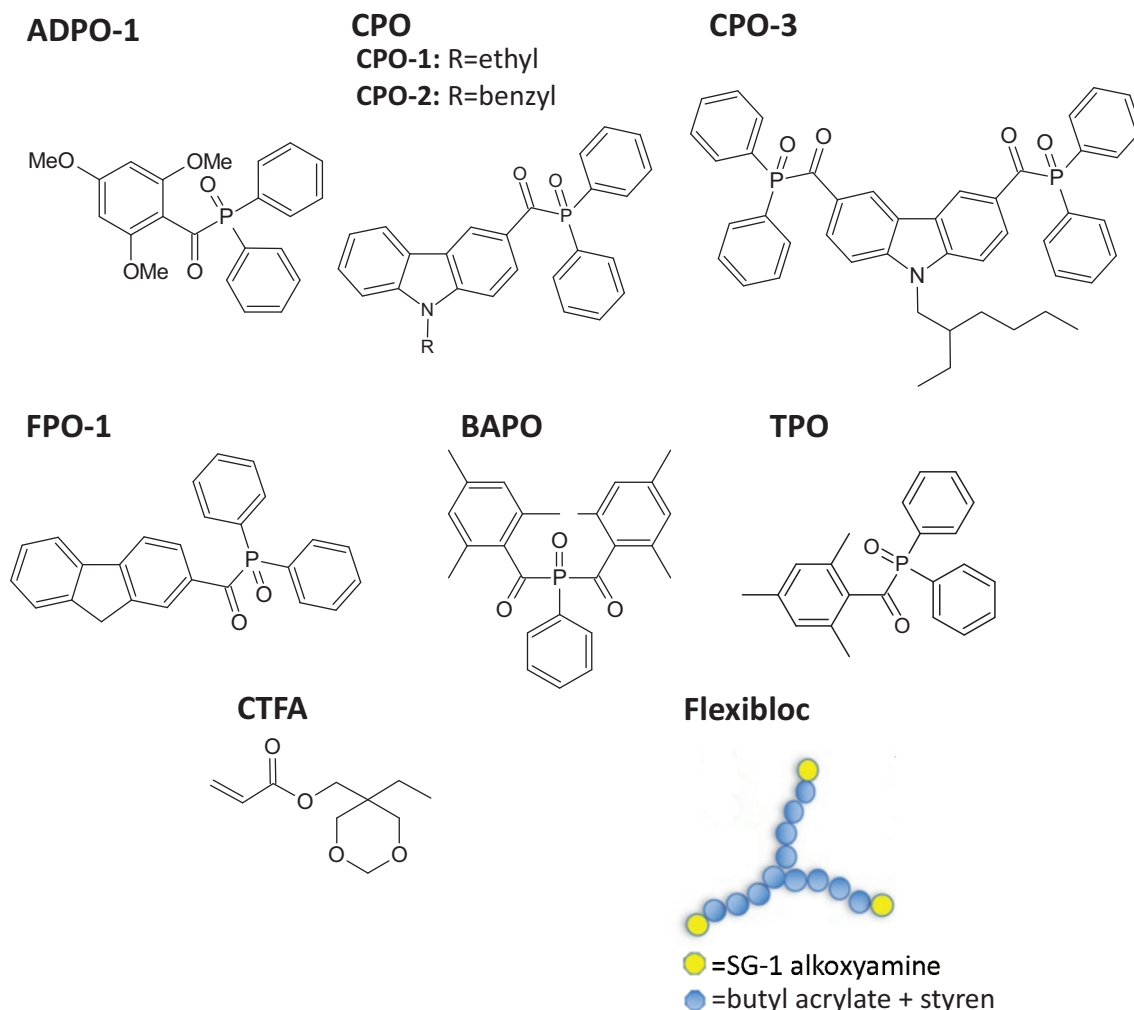
During photopolymerization, a liquid system, consisting of a monomer/oligomer and a photoinitiator, is irradiated to form a solid polymer.¹² Thus, in photopolymerization two factors are particularly important: the irradiation wavelength and the photoinitiator efficiency. During the development of light curing and 3D printing, the wavelengths chosen to initiate the polymerization were in the UV range.^{13,14} However, these wavelengths have several disadvantages such as poor light penetration into the resins,¹⁵ slower 3D printing rate, and high toxicity to the skin and DNA,¹⁶ caused by the high energy photons emitted at these wavelengths. In order to have a safer and more efficient irradiation, the near UV (405 nm) and the visible light are increasingly privileged to initiate the photopolymerization,¹⁷ which allow the use of this polymerization method in various medical fields such as hydrogel, adhesive, and dentistry.^{13,18–20}

Besides, in the general field of photopolymerization another key factor in light curing is the selection of a suitable photoinitiator. When subjected to adequate irradiation, it generates active species which initiate polymerization.¹² For the photopolymerization to be effective, it is crucial that the initiating system has good absorbance at the irradiation wavelength. Currently, with the increasing use of near UV and visible light to initiate photopolymerization, the search for photoinitiators that allow polymerization at these longer wavelengths, has seen a significant increase in interest.²¹

One of the most studied families of photoinitiators is the phosphine oxides. In particular, acyldiphenylphosphine oxides generally have a good absorbance between 350 and 400 nm ($\epsilon > 500 \text{ L mol}^{-1} \text{ cm}^{-1}$) and allow the generation of highly reactive phosphinoyl and acyl radicals,²² which makes them particularly interesting compounds in the context of photopolymerization. Furthermore, as the absorbance band of acyldiphenylphosphine oxides is relatively broad and extends to 400 nm,¹² it is promising to further improve their absorption properties in the visible range by considering new derivatives. For this purpose, several modifications of phosphine oxides have already been proposed whether by changing the nature of the acyl group,^{23,24} (e.g., CPO-1 has found interesting reactivity in photopolymerization, see Scheme 1)²⁵ or the nature of the substituents on the phosphorus.^{26,27} The corresponding phosphine oxides were successfully used for photopolymerization under LEDs.^{23–26}

Another advantage of changing the nature of the phosphine oxides is to limit their migration to the surface of the materials after polymerization. Indeed, this type of leaching is problematic when using photopolymerisable resins in food packaging materials or those in direct contact with the human body.²⁸ In addition, commercial photoinitiators, such as BAPO or TPO, have shown relatively high toxicity.²⁹ As a consequence, the migration of unreacted photoinitiators can lead to problems of contamination or toxicity. The search for photoinitiators with a lower hazard level is therefore essential. Currently, two methods are being studied to limit the migration of photoinitiators.³⁰ Either by adding polymerisable functions to the photoinitiators, so that they participate in the photopolymerization and are trapped in the materials,^{30,31} or by adding massive groups to the photoinitiators to limit their diffusion in the polymers (e.g., macromolecular photoinitiators).³² Thus, the modification of phosphine oxides has these two interests. It is therefore crucial to study the effects of structural variations on the final properties of photoinitiators.

In this work, based on molecular design through molecular orbitals calculation, we propose to focus our attention on novel acyldiphenylphosphine oxides bearing various (hetero)aroyl groups. Initially, the physical properties (triplet energy, bond dissociation energy, cleavage reaction enthalpy, and absorption properties) of numerous acyldiphenylphosphine oxides were calculated by molecular modeling. Then, the four most promising compounds were prepared, their absorption properties were measured. Moreover, their efficiencies for photopolymerizations, in a blend of cyclic trimethylolpropane formal acrylate (CTFA)/Flexibloc under the LED irradiation at 405 nm were evaluated. Herein, the Flexibloc was added



SCHEME 1 Structure of the compounds involved in this study. [Color figure can be viewed at wileyonlinelibrary.com]

to control the viscosity of the resin. In this context, diphenylphosphine oxides bearing 2,4,6-trimethoxyphenyl (ADPO-1), carbazole (CPO-2 and CPO-3), and fluorene (FPO-1) aryl groups were studied. To the best of our knowledge, these photoinitiators have never been reported for 3D printing. Markedly, CPO-3 and FPO-1 have never been synthesized before. Furthermore, the cytotoxicity of one of the synthesized compounds, ADPO-1 with high storage stability, was tested which showed significantly lower cytotoxicity than one of the benchmark photoinitiator TPO (Scheme 1).

Almost all the photosensitive resins developed for VAT photopolymerization 3D printing techniques (SLA, DLP...) lead to thermosetting materials (e.g., using multifunctional (meth)acrylate monomers). The use of monofunctional monomers is much scarce, but can lead to thermoplastic polymers that have the advantage of being easier to recycle (by melting). However, monofunctional

monomers usually have low viscosities that need to be adapted for good printability, that is., monofunctional monomers are often used as reactive diluent and combined with other multifunctional monomers or oligomers.³³ In this work, flexiblocs were used for this purpose, even though they have been reported as potential initiators of nitroxide-controlled radical polymerization by the thermal route. In our case, this latter property of flexiblocs was not used and photopolymerization is not expected to be controlled.

2 | RESULTS AND DISCUSSION

2.1 | Molecular design

Initially, the properties of various acyldiphenylphosphine oxides were calculated by molecular modeling. Several

criteria must be fulfilled before the corresponding acyldiphenylphosphine oxides were synthesized. First, the acyldiphenylphosphine oxide should present an absorption maximum in the UV or near UV. Second, the cleavage reaction of the C—P bond must be favorable and therefore have a negative bond cleavage enthalpy (ΔH ; $\Delta H = BDE - E_T$; with: BDE the bond dissociation energy and E_T the energy of the triplet state) or close to 0 Kcal mol⁻¹. It should be noted that, with the level of theory used, B3LYP/6-31G*, an uncertainty exists. Therefore, for structures giving slightly positive ΔH values it is possible that the cleavage reaction remains favorable. The last parameter that has been evaluated is the spin density around the formed radicals (P[•] and C[•]). Indeed, the more the spin density is delocalized, the more the radicals are stable and therefore, they are less reactive. Finally, by considering these properties, all four acyldiphenylphosphine oxides seem promising and were selected for further study (Table 1): ADPO-1, CPO-2, CPO-3, and FPO-1 (Scheme 1). It is noteworthy that only ADPO-1, CPO-1, and CPO-2 have already been reported by our group^{23,25} but their use has been limited to photopolymerizations under LED irradiation at 395 nm and they were never applied for 3D printing. Compounds CPO-3 and FPO-1 were prepared for the first time therein and used successfully in photopolymerization.

2.2 | Syntheses of photoinitiators (ADPO-1, CPO-2, CPO-3, and FPO-1)

Photoinitiators CPO-2 and ADPO-1 were initially prepared following a fast and efficient two steps procedure already described by our group^{23,25}: (1) nucleophilic addition of a phosphine oxide to an aromatic aldehyde in the presence of Na₂CO₃ without solvent to afford a secondary alcohol that required no further purification and could directly be reacted further; (2) oxidation of the secondary alcohol to the corresponding ketone in the presence of MnO₂ (Scheme 2). This procedure afforded compounds CPO-2 and ADPO-1 in good two steps isolated yields of 81% and 93% respectively.

However, during the preparation of compound CPO-3, the expected diol was not obtained under the

classical conditions described above. Indeed, the addition of two equivalents of diphenylphosphine oxides on the 9-(2-ethylhexyl)carbazole-3,6-dicarboxaldehyde (1 equivalent per aldehyde function), afforded a complex crude reaction mixture. Therefore, the reaction conditions have been reoptimized. It turned out that the addition of 5 equivalents of diphenylphosphine oxide gave the desired diol with a 70% yield.

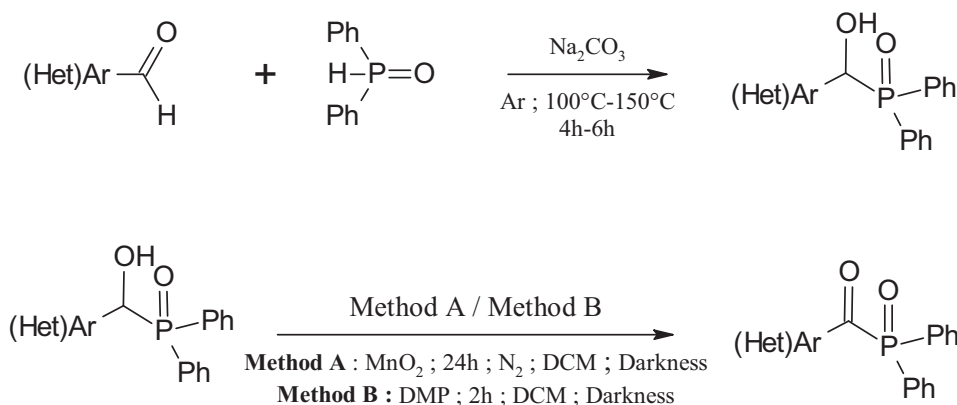
Thereafter, during the preparation of the compounds CPO-3 and FPO-1 difficulties were encountered: the nucleophilic addition afforded the desired alcohols in yields of 70% for CPO-3 and 91% for FPO-1. But, the oxidation of the secondary alcohols in the presence of MnO₂ did not give the expected photoinitiators. Indeed, at the end of the reaction, only the alcohols were recovered unchanged. It was therefore necessary to reoptimize the conditions and develop a new oxidation method for both alcohols. For this purpose, MnO₂ was replaced by the Dess Martin periodinane (DMP).³⁴ Gratifyingly, the photoinitiators CPO-3 and FPO-1 were successfully obtained with overall yields of 63% and 78%, respectively (Scheme 2). It should be noted that, the oxidation with DMP was also evaluated for the preparation of CPO-2 and it proved to be more effective than the one with MnO₂: CPO-2 was obtained with a better 93% isolated yield (81% using MnO₂ as the oxidizing agent) (Scheme 2).

2.3 | Absorption properties of the synthesized photoinitiators

Subsequently, the four new photoinitiators were characterized by UV–visible spectroscopy. A crucial aspect in the development of new light-sensitive molecules for photopolymerization is their ability to absorb light at the irradiation wavelength. The UV–visible absorbance spectra of the synthesized structures were determined between 325 and 600 nm in acetonitrile and compared to the absorbance spectrum of the BAPO (Figure 1). It was observed that CPO-2 and CPO-3 showed relatively similar absorbance spectra, and they had a better absorption than all other photoinitiators including the commercially available BAPO. Looking specifically at the absorbance at 405 nm, CPO-2 ($\epsilon_{405\text{nm}} = 1330 \text{ L mol}^{-1} \text{ cm}^{-1}$) and

Molecules	λ_{max} (nm)	E_t (kcal mol ⁻¹)	BDE (kcal mol ⁻¹)	ΔH (kcal mol ⁻¹)
ADPO-1	373	60	58	-2
CPO-2	385	61	62	1
CPO-3	390	60	61	1
FPO-1	402	57	62	4

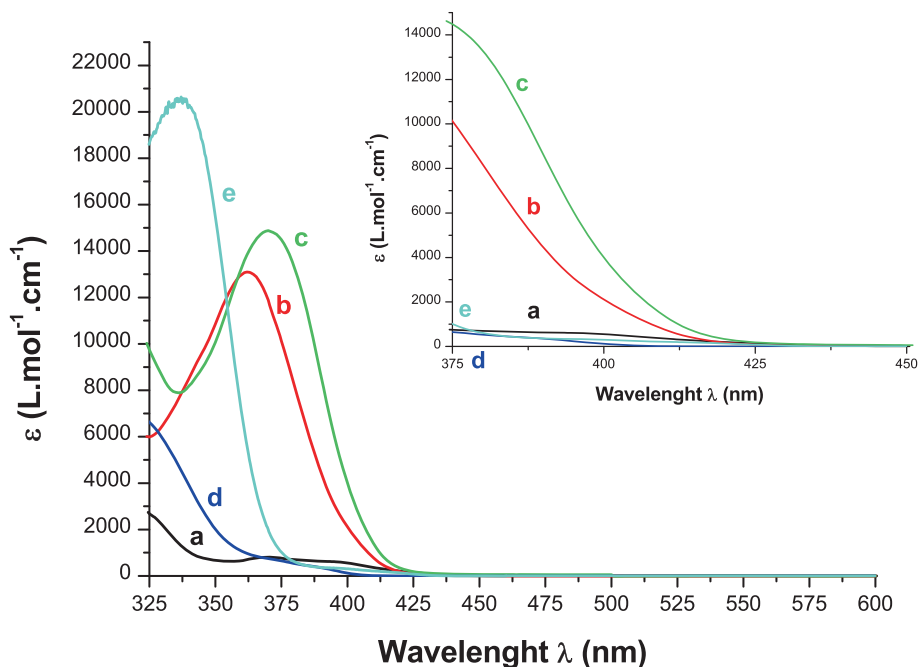
TABLE 1 Predicted properties: Light absorption maximum (λ_{max}), triplet state energy (ET), bond dissociation energy (BDE) for the C—P bond, enthalpy for the cleavage process from T1 (ΔH).



Photoinitiators	Method (A or B)	Isolated Yield (2 steps)
ADPO-1	A	93%
CPO-2	A	81%
	B	91%
CPO-3	B	63%
FPO-1	B	78%

SCHEME 2 General route to acyldiphenylphosphines photoinitiators, yields and methods used are given in the table.

FIGURE 1 UV-visible spectra in acetonitrile of the (a) BAPO, (b) CPO-2, (c) CPO-3, (d) ADPO-1, and (e) FPO-1. [Color figure can be viewed at wileyonlinelibrary.com]



CPO-3 ($\epsilon_{405\text{nm}} = 1430 \text{ L mol}^{-1} \text{ cm}^{-1}$) had an absorbance at least twice as high as that of the BAPO ($\epsilon_{405\text{nm}} = 500 \text{ L mol}^{-1} \text{ cm}^{-1}$). However, the absorptions

of ADPO-1 and FPO-1 were lower than that of BAPO at 405 nm ($\epsilon_{405\text{nm}} = 50$ and $\epsilon_{405\text{nm}} = 290 \text{ L mol}^{-1} \text{ cm}^{-1}$ for ADPO-1 and FPO-1, respectively) (Table 2).

2.4 | Photoinitiation efficiency of the new photoinitiators in photopolymerization

Once their absorbances were determined, the reactivity of the different compounds was evaluated. To this end, photopolymerizations of resins containing the different photoinitiators, the Flexibloc, which was added to control the viscosity of the resin, and an acrylic monomer, cyclic trimethylolpropane formal acrylate (CTFA), were monitored using RT-FTIR. To initiate the polymerization, a 405 nm LED with a power of 170 mW/cm² was used. All the photopolymerizations were done for 2 mm thick samples under air. BAPO, being commercially available, served as a reference in order to determine the effectiveness of photoinitiators in photopolymerization and 3D printing.

2.4.1 | With 0.1 wt% of photoinitiators in the resins

At first, polymerizations for resin containing 0.1 wt% photoinitiator were carried out. Under these conditions, it appeared that the resin containing BAPO gave a better

kinetic and final conversion (90%) than the other photoinitiators (Figure 2). CPO-2 and CPO-3 demonstrated similar reactivity (final conversion = 32%) and lower initiation rates than the ADPO-1. For this compound, there appeared to be an induction time before the polymerization began. This was linked to the inhibition by the oxygen present in the resin, which must be consumed before the polymerization reaction began. However, ADPO-1 achieved much higher final conversions than the other synthesized products (85%). Finally, FPO-1 led to very slow polymerization kinetics and can only achieve low conversion (18%).

2.4.2 | With 1 wt% of photoinitiators in the resins

Polymerizations for resins containing 1% photoinitiators were also carried out (Figure 3). BAPO, CPO-2, CPO-3, and ADPO-1 can initiate the photopolymerization and lead to similar final conversions (>95%) of polymerization. FPO-1 had a lower reactivity than the other compounds and gave a lower final conversion (80%). In regards to the polymerization rate ($R_p/[M_0] \times 100$), CPO-2 ($(R_p/[M_0]) \times 100 = 6.94 \text{ s}^{-1}$) as well as ADPO-1

Molecules	ADPO-1	CPO-2	CPO-3	FPO-1	BAPO
$\epsilon_{405\text{nm}}$ (L mol ⁻¹ cm ⁻¹)	50	1330	1430	290	500

TABLE 2 Extinction coefficients (ϵ) of the different photoinitiators at 405 nm.

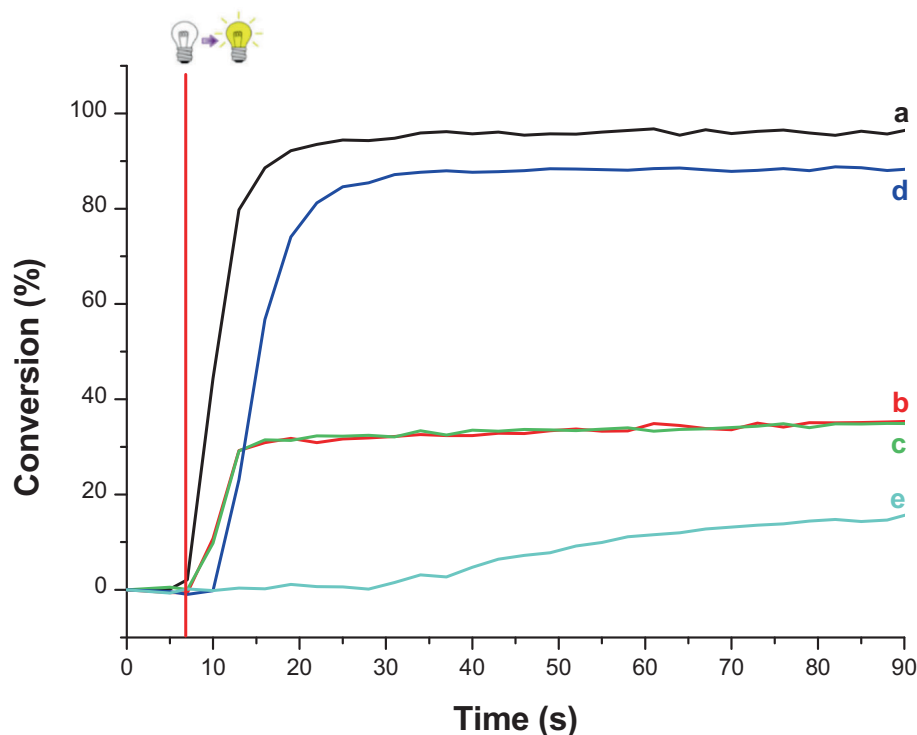


FIGURE 2 Photopolymerization kinetics (acrylate conversion vs. irradiation time) for the resins containing 10 wt% copolymer + 89.9 wt% CTFA monomer in the presence of the different photoinitiators (0.1 wt%): (a) BAPO, (b) CPO-2, (c) CPO-3, (d) ADPO-1, and (e) FPO-1. [Color figure can be viewed at wileyonlinelibrary.com]

$((R_p/[M_0]) \times 100 = 12.94 \text{ s}^{-1})$ demonstrated a higher rate than BAPO ($((R_p/[M_0]) \times 100 = 4.93 \text{ s}^{-1})$) and CPO-3 ($((R_p/[M_0]) \times 100 = 4.14 \text{ s}^{-1})$), the latter having slightly lower initiation kinetics than BAPO. Although ADPO-1 had a lower absorption than the other initiators, it was more effective in photopolymerization. This difference in effectiveness was due to the stability of the formed radicals for CPO-2 and CPO-3. Because of the carbazole

group, the radicals formed by CPOs were more stable than those generated from ADPO-1, which resulted in this lower reactivity. The lower efficiency of the BAPO-containing resin versus ADPO-1 can be caused by an inner filter effect (the optical densities in the film are much higher for BAPO versus ADPO-1: 2.4 and $A_{ADPO-1} = 0.25$, respectively). Indeed, by increasing the concentration of photoinitiator, the absorbance in the sample

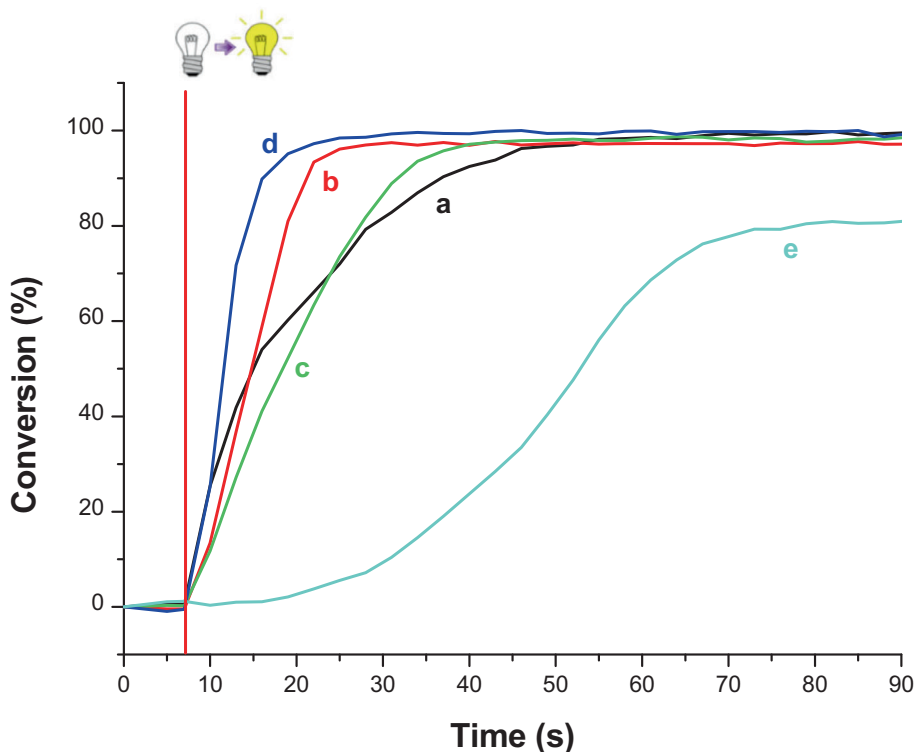


FIGURE 3 Photopolymerization kinetics (acrylate conversion vs. irradiation time) for resins containing 10 wt% copolymer + 89 wt% CTFA monomer in the presence of the different photoinitiators (1 wt%): (a) BAPO, (b) CPO-2, (c) CPO-3, (d) ADPO-1, and (e) FPO-1. [Color figure can be viewed at wileyonlinelibrary.com]

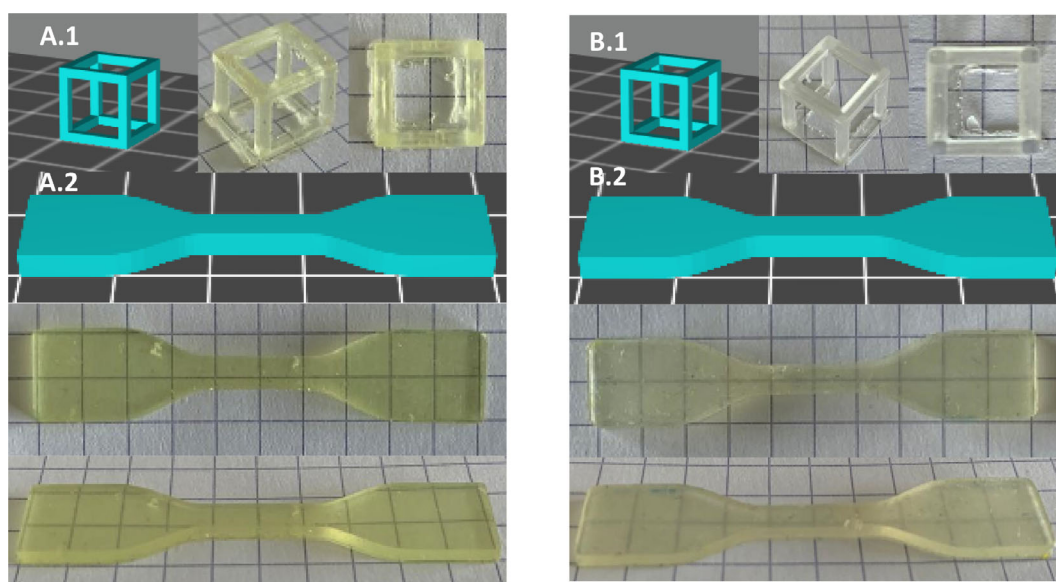


FIGURE 4 Pictures of 3D printed objects using: BAPO [A.1] a hollow cube of 1 cm on each side [A.2] specimen for tensile tests and CPO-2 [B.1] a hollow cube of 1 cm on each side [B.2] specimen for tensile. [Color figure can be viewed at wileyonlinelibrary.com]

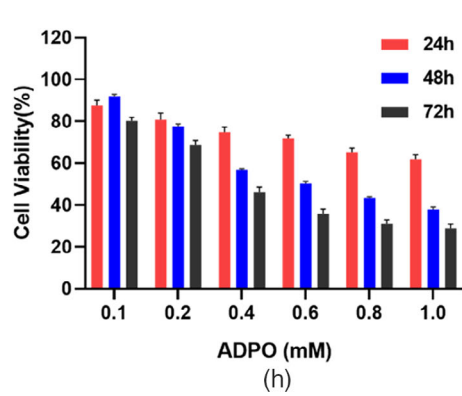
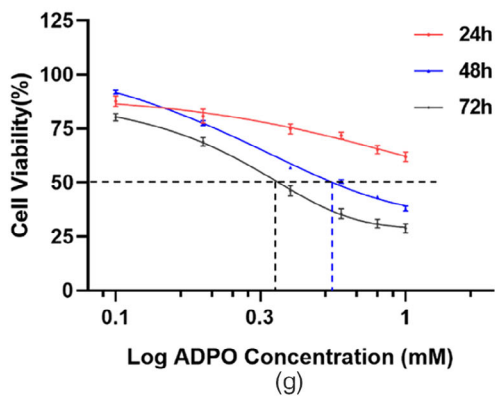
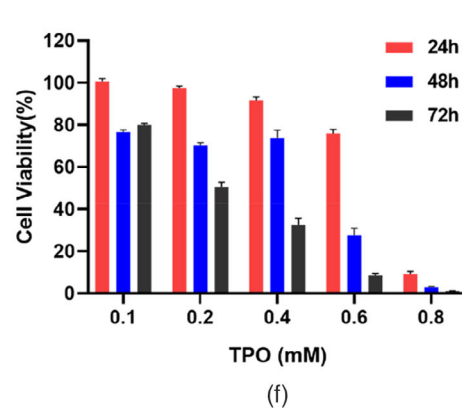
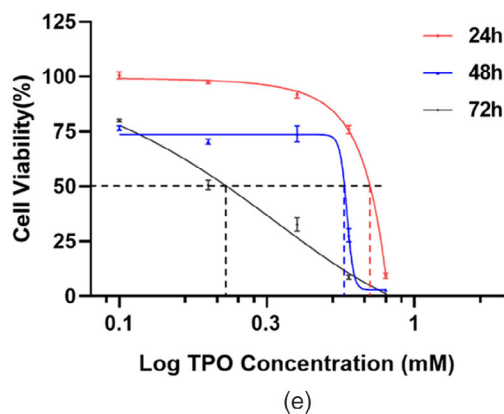
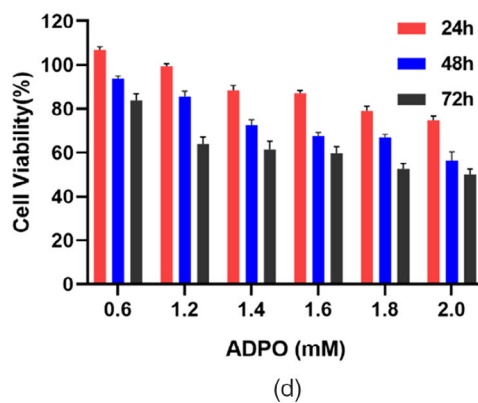
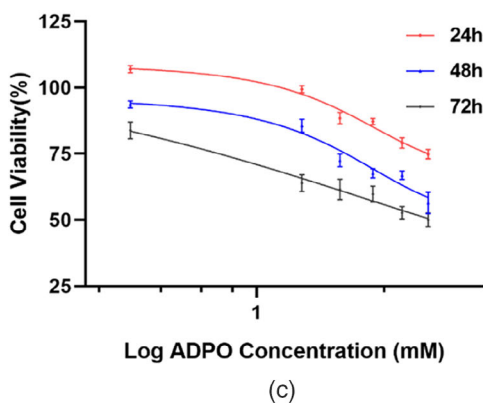
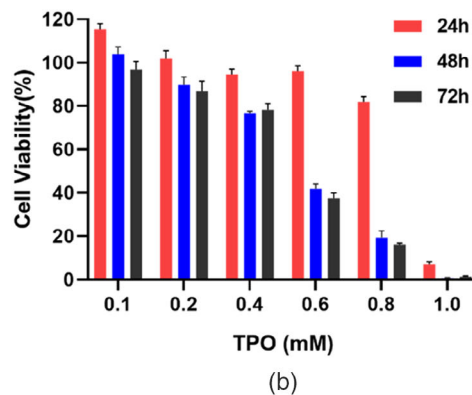
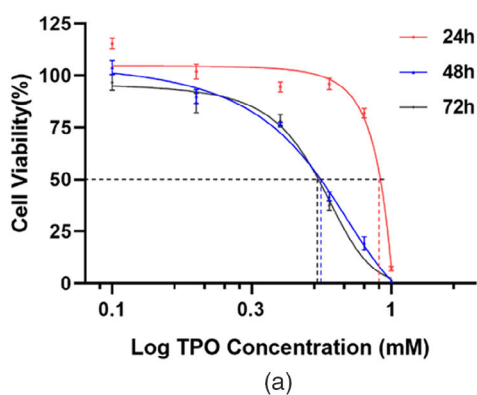


FIGURE 5 In vitro cytotoxicity of ADPO-1 and TPO in human umbilical vein endothelial cells (HUVECs) (a–d) and Human normal hepatocytes (L02) (e–h) after 24, 48, and 72 h of incubation. [Color figure can be viewed at wileyonlinelibrary.com]

increases. As a result, the irradiation of the deepest areas of the sample was more difficult, which led to a decrease in reactivity.

2.5 | Storage stability of the synthesized photoinitiators

Another key point is the stability of the photoinitiators during storage. For this purpose, the different photoinitiators were stored under argon and protected from light at 4°C. Then, ¹H NMR analyses of photoinitiators were performed once a month. The degradation of the photoinitiator was observed by looking at the appearance of a signal at 7.76 ppm which corresponded to the reformation of the diphenylphosphine oxide (Ph₂P(=O)H) used as starting material in the nucleophilic addition step. Among the 4 synthesized compounds, only ADPO-1 showed an excellent stability: indeed, no degradation was observed even after 12 months of storage. CPO-2 showed degradation after 2 months of storage and therefore had a moderate stability. Unfortunately, CPO-3 and FPO-1 showed a poor stability since they were totally degraded after only 1 month of storage.

2.6 | 3D printing using the synthesized photoinitiators

Finally, the efficiency of the proposed photoinitiators was evaluated in 3D printing. To carry out these experiments, a low intensity LCD screen 3D printer was chosen. With a very low viscosity for CTFA (13–15 mPa.s),³³ it is not easy to print it directly. Therefore, Flexibloc was added in the photosensitive resin to improve printability. Due to the low irradiation intensity of the screen (0.8 mW/cm²), only photoinitiators with a high reactivity can be used to obtain well defined objects. The CPO-2 and ADPO-1 photoinitiators, which were stable in the monomer, were therefore used in these printing experiments. 3D printing was also performed for a resin containing BAPO for the comparison. First, the tests were carried out on a relatively simple object: a specimen for tensile tests (Figure 4A.2 and B.2). The printing experiments worked with CPO-2 and BAPO for similar layer irradiation time (≈15 s with BAPO and CPO-2) (Figure 4). However, 3D printing cannot work using ADPO-1. Because of its weak absorption at 405 nm and the low intensity of the irradiation, ADPO-1 cannot generate enough initiating radicals to consume the oxygen present in the resin, which explained the impossibility of obtaining a 3D printed object. In order to get a better idea of the reactivity of the resins, 3D printing experiments were

made for a more complex object: a hollow cube of 1 cm on each side (Figure 4A.1 and B.1). For this model, both BAPO and CPO-2 allowed to obtain a perfectly printed object. For these experiments, the irradiation time for each layer was the same as before (≈15 s) for the two photoinitiators. This was consistent with the results obtained from the RT-FTIR experiments, where CPO-2 showed the reactivity similar to BAPO. Thus, the two resins tested in 3D printing demonstrated good efficiency. Finally, among the synthesized photoinitiators, only CPO-2 allowed to obtain 3D printed objects.

2.7 | Cytocompatibility of the synthesized photoinitiators

2.7.1 | In vitro cytocompatibility of ADPO-1

With the increasing use of photoinitiators, their cytocompatibility became of major interest. Because of its excellent storage, it was important to evaluate the cytotoxicity of ADPO-1. To this end, MTT assay was performed to assess the in vitro cytotoxicity of ADPO-1 in both HUVECs (human umbilical vein endothelial cells) and L02 (human normal hepatocytes) cells using a commercially available photoinitiator, TPO as a control which was also known to have a relatively high cytotoxicity.²⁹ The cytocompatibility of BAPO has been already investigated in Reference 29. Toxicity of BAPO is higher than for TPO. That is the reason why TPO was selected in this work for toxicity investigation. The well tolerance of ADPO-1 by HUVECs was supported by the cell viabilities above 50% at all evaluated concentrations in a range from 0.6 to 2 mM (Figure 5c, d). In contrast, the IC₅₀ (=50% inhibiting concentration) values of TPO were determined to be 0.87, 0.54, and 0.53 mM for 24, 48, and 72 h of incubation, respectively. Similar trend was observed in L02 cells, that is, ADPO-1 showed consistently much lower cytotoxicity than TPO (Figure 5e–h). Interestingly, both photoinitiators mediated greater cytotoxicity in L02 cells than in HUVECs, which was likely attributed to the cell type-dependent cytotoxicity. The overall results confirmed the significantly better biocompatibility of ADPO-1 than that of TPO.

3 | CONCLUSION

Short and efficient routes to novel photoinitiators belonging to the family of phosphine oxides were developed. Among these compounds, CPO-2 and ADPO-1 were respectively 1.5 and 3 times more efficient than BAPO in terms of polymerization kinetics. In addition, during

storage, ADPO-1 showed excellent stability, which was not the case for the other photoinitiators. As a result, only the cytotoxicity of ADPO-1 was evaluated and was found to be relatively low compared to that of TPO. Finally, only the CPO-2 photoinitiator allowed printing complex objects while requiring short irradiation time (≈ 15 s per layer) using the 3D printer with a very low intensity of irradiation source. Other low toxicity Types I photoinitiators will be studied in forthcoming work.

4 | MATERIALS AND METHODS

4.1 | Photoinitiators syntheses

All reagents were purchased from Aldrich and TCI and were used as received without further purification. Activated MnO_2 was purchased from Aldrich. The first step of the syntheses of photoinitiators (nucleophilic addition of diphenylphosphine oxide on aldehydes) were carried out under an atmosphere of argon. The second step (oxidation reactions of the secondary alcohols to ketones) was carried out in dichloromethane (DCM) and in the dark to avoid any degradation of the final products due to ambient light.

The ^1H , ^{31}P , and ^{13}C NMR spectra were obtained at room temperature with a Varian Oxford 300 spectrometer.

4.2 | Synthesis of ADPO-1

Step 1: 2,4,6-trimethoxybenzaldehyde (4 mmol, 0.785 g, 1 equiv.), diphenylphosphine oxide (4.2 mmol, 0.850 g, 1.05 equiv.), and Na_2CO_3 (4.2 mmol, 0.445 g, 1.05 equiv.) were introduced into a 5 mL round bottom flask without solvent. The reaction medium was purged three times with argon, placed under an argon atmosphere, stirred and heated to 140°C for 4 h. The reaction medium was then dissolved in 50 mL of DCM and washed with 50 mL of distilled water. After extraction, the organic layer was dried over anhydrous MgSO_4 then the solvent was removed under reduced pressure. The crude reaction mixture was then dried under vacuum for 2 h. A white solid was obtained (1.5138 g, 95% isolated yield) and directly used in step 2 without further purification. $^1\text{H-NMR}$ (CDCl_3) δ (ppm): 7.92–7.86 (m, 2H), 7.76–7.70 (m, 2H), 7.52–7.31 (m, 6H), 6.12–6.06 (m, 1H), 6.00 (s, 2H), 4.66–6.62 (d, $J = 12$ Hz, 1H) 3.77 (s, 3H), 3.49 (s, 6H). $^{31}\text{P-NMR}$ (CDCl_3) δ (ppm): 28.42. $^{13}\text{C-NMR}$ (CDCl_3) δ (ppm):

55.3, 55.6, 67.6 (d, $J = 82.7$ Hz), 90.6, 104.5, 127.8 (d, $J = 11.3$ Hz), 128.1 (d, $J = 11.3$ Hz), 131.2 (d, $J = 2.5$ Hz), 131.3, 131.4 (d, $J = 5.0$ Hz), 132.2 (d, $J = 7.6$ Hz), 132.8 (d, $J = 92.0$ Hz), 133.0 (d, $J = 93.2$ Hz), 159.1, 159.2, 161.4. HRMS: m/z calcd for $\text{C}_{22}\text{H}_{23}\text{O}_5\text{P}$ ($\text{M} + \text{Na}^+$): 398.3887, found: 398.1283.

Step 2 (method A): The alcohol obtained in step 1 (1.25 mmol, 0.500 g, 1 equiv.), was dissolved in DCM (25 mL) in a 50 mL round bottom flask and activated MnO_2 (25 mmol, 2.1823 g, 20 equiv.) was added in one portion. The reaction medium was purged three times with argon, placed under an argon atmosphere and stirred in the dark for 18 h. The reaction mixture was then filtered over celite. The filtrate was concentrated under reduced pressure. A yellow gum was obtained (0.4883 g, 98% isolated yield) and used without further purifications for photopolymerizations. $^1\text{H-NMR}$ (CDCl_3) δ (ppm): 7.88–7.82 (m, 4H), 7.54–7.44 (m, 6H), 6.09 (s, 2H), 3.83 (s, 3H), 3.64 (s, 6H). $^{31}\text{P-NMR}$ (CDCl_3) δ (ppm): 17.34. HRMS: m/z calcd for $\text{C}_{22}\text{H}_{21}\text{O}_5\text{P}$ ($\text{M} + \text{Na}^+$): 396.3729, found: 396.1127. The $^1\text{H-NMR}$, $^{31}\text{P-NMR}$, spectra were in accordance with a previous report.²³

4.3 | Synthesis of CPO-2

Step 1: 9-benzyl carbazole-3-carboxaldehyde (1.75 mmol, 0.500 g, 1 equiv.), diphenylphosphine oxide (1.92 mmol, 0.389 g, 1.1 equiv.), and Na_2CO_3 (1.92 mmol, 0.204 g, 1.1 equiv.) were introduced into a 5 mL round bottom flask without solvent. The reaction medium was purged three times with argon, placed under an argon atmosphere, stirred and heated to 120°C for 1 h then 100°C for 5 h. The reaction medium was then dissolved in 200 mL of DCM and washed with 200 mL of distilled water. After extraction, the organic layer was dried over anhydrous MgSO_4 then the solvent was removed under reduced pressure. The crude reaction mixture was then dried under vacuum for 2 h. A white solid was obtained (0.8105 g, 95% isolated yield) and directly used in step 2. $^1\text{H-NMR}$ (CDCl_3) δ (ppm): 7.95–7.82 (m, 4H), 7.71–7.08 (m, 18H), 5.67 (m, 1H), 5.48 (s, 2H), 3.44–3.42 (m, 1H). $^{31}\text{P-NMR}$ (CDCl_3) δ (ppm): 27.51. $^{13}\text{C-NMR}$ ($\text{C}_5\text{D}_5\text{N}$) δ (ppm): 46.8, 74.9 (d, $J = 86.7$ Hz), 109.2, 110.0, 120.0, 120.9, 121.1, 123.4, 126.6, 127.0, 127.2, 128.0, 128.7 (d, $J = 11.3$ Hz), 129.0 (d, $J = 11.3$ Hz), 129.4, 130.4, 132.1 (d, $J = 2.5$ Hz), 132.2 (d, $J = 2.5$ Hz), 132.7 (d,

$J = 7.6$ Hz), 132.9, 133.5 (d, $J = 7.6$ Hz), 134.9 (d, $J = 92.0$ Hz), 136.2, 138.3, 141.1, 141.7. HRMS: m/z calcd for $C_{32}H_{26}NO_2P$ ($M + Na^+$): 487.5281, found: 487.1701.

Step 2 (method A): The alcohol obtained in step 1 (1.3 mmol, 0.630 g, 1 equiv.), was dissolved in DCM (75 mL) in a 50 mL round bottom flask and activated MnO_2 (26 mmol, 2.604 g, 20equiv.) was added in one portion. The reaction medium was purged with three times argon and placed under an argon atmosphere and stirred in the dark for 24 h. The reaction mixture was then filtered over celite. The filtrate was concentrated under reduced pressure. An orange gum was obtained (0.5365 g, 85% isolated yield) and used without further purifications for photopolymerizations. 1H -NMR ($CDCl_3$) δ (ppm): 8.66–8.63 (d, $J = 10$ Hz, 1H), 8.24–8.22 (d, $J = 10$ Hz, 1H), 7.99–7.92 (m, 4H), 7.57–7.11 (m, 14H), 5.54 (s, 2H). ^{31}P -NMR ($CDCl_3$) δ (ppm): 22.53. HRMS: m/z calcd for $C_{32}H_{25}NO_2P$ ($M + Na^+$): 485.5122, found: 485.154. The 1H -NMR, ^{31}P -NMR, spectra were in accordance with a previous report.²⁵

Step 2 (method B): The alcohol obtained in step 1 (0.2 mmol, 0.100 g, 1 equiv.), was dissolved in DCM (0.8 mL) in a 5 mL round bottom flask and DMP (0.3 mmol, 0.1272 g, 1.5 equiv.) was added in three portion. The reaction medium was stirred in the dark for 2 h. The reaction mixture was then quenched with 3 mL of Na_2SO_3 . The resulting mixture was extracted with 20 mL of DCM, then the combine organics layers were washed with 20 mL of saturated aqueous Na_2SO_3 and 20 mL of saturated aqueous $NaHCO_3$. After extraction, the organic layer was dried over $MgSO_4$ then, the solvent was removed under reduced pressure. The crude reaction mixture was then dried under vacuum for 2 h. An orange gum was obtained (0.0903 g, 93% isolated yield) and used without further purifications for photopolymerizations. The 1H -NMR, ^{31}P -NMR, spectra were in accordance with the results obtained using method A and with a previous report.²⁵

4.4 | Synthesis of CPO-3

Step 1: 9-(2-ethylhexyl)carbazole-3,6-dicarboxaldehyde (0.6 mmol, 0.200 g, 1 equiv.), diphenylphosphine oxide (3 mmol, 0.389 g, 5 equiv.), and Na_2CO_3 (3 mmol, 0.318 g, 5 equiv.) were introduced into a 5 mL round bottom flask without solvent. The reaction medium was purged three times with argon, placed under an argon atmosphere, stirred and heated to 150°C for 1 h then 120°C for 5 h. The

reaction medium was then dissolved in 150 mL of DCM and washed with 150 mL of distilled water. After extraction, the organic layer was dried over anhydrous $MgSO_4$ then the solvent was removed under reduced pressure. The obtained solid was washed with 200 mL of diethyl ether to remove the excess of phosphine. The crude reaction mixture was then dried under vacuum for 4 h. A yellow solid was obtained (0.3062 g, 69% isolated yield) and directly used in step 2. 1H -NMR ($CDCl_3$) δ (ppm): 7.79–7.10 (m, 26H), 5.58–5.57 (m, 2H), 4.04–4.0 (m, 2H) 1.94 (s, 1H), 1.38–1.21 (m, 8H), 0.83–0.85 (m, 6H). ^{31}P -NMR ($CDCl_3$) δ (ppm): 31.33. HRMS: m/z calcd for $C_{46}H_{47}NO_4P_2$ ($M + NH_4^+$): 739.8172, found: 739.2980.

Step 2 (method B): The alcohol obtained in step 1 (0.14 mmol, 0.100 g, 1 equiv.), was dissolved in DCM (0.56 mL) in a 5 mL round bottom flask and DMP (0.42 mmol, 0.1781 g, 3 equiv.) was added in three portion. The reaction medium was stirred in the dark for 2 h. The reaction mixture was then quenched with 3 mL of Na_2SO_3 . The resulting mixture was extracted with 20 mL of DCM, then the combine organics layers were washed with 20 mL of saturated aqueous Na_2SO_3 and 20 mL of saturated aqueous $NaHCO_3$. After extraction, the organic layer was dried over $MgSO_4$ then, the solvent was removed under reduced pressure. The crude reaction mixture was then dried under vacuum for 2 h. An orange solid was obtained (0.0895 g, 90% isolated yield) and used without further purifications for photopolymerizations. 1H -NMR ($CDCl_3$) δ (ppm): 9.3 (s, 2H), 8.91–8.88 (d, $J = 15$ Hz, 2H), 7.98–7.92 (m, 8H), 7.58–7.43 (m, 14H), 4.20–4.14 (m, 2H) 1.63 (br s, 1H), 1.43–1.26 (m, 8H), 0.92–0.84 (m, 6H). ^{31}P -NMR ($CDCl_3$) δ (ppm): 22.53. ^{13}C -NMR ($CDCl_3$) δ (ppm): 10.8, 14.0, 22.9, 24.3, 28.8, 30.9, 39.4, 47.9, 109.7, 123.5, 124.3, 128.6 (d, $J = 12.6$ Hz), 129.6, 130.3 (d, $J = 73.1$ Hz), 130.5 (d, $J = 73.1$ Hz), 131.9 (d, $J = 10.1$ Hz), 132.1, 132.3 (d, $J = 2.5$ Hz), 145.4, 202.5 (d, $J = 82$ Hz). HRMS: m/z calcd for $C_{46}H_{43}NO_4P_2$ ($M + H^+$): 735.7854, found: 735.2667.

4.5 | Synthesis of FPO-1

Step 1: 2-fluorène-carboxaldehyde (1.06 mmol, 0.210 g, 1 equiv.), diphenylphosphine oxide (1.14 mmol, 0.230 g, 1.06 equiv.), and Na_2CO_3 (1.07 mmol, 0.123 g, 1.16 equiv.) were introduced into a 5 mL round bottom flask without solvent. The reaction medium was purged three times with argon, placed

under an argon atmosphere, stirred and heated to 100°C for 4 h. The reaction medium was filtered under vacuum, the obtained solid was washed with 25 mL of distilled water and then 20 mL of ethyl acetate. The crude reaction mixture was then dried under vacuum for 4 h. A white solid was obtained (0.408 g, 97% isolated yield) and directly used in step 2. ¹H-NMR (DMSO-*D*₆) δ (ppm): 7.81–7.69 (m, 6H), 7.59–7.21 (m, 11H), 6.57 (s, 1H), 5.71–5.70 (d, *J* = 10 Hz, 1H), 3.79 (s, 2H). ³¹P-NMR (DMSO-*D*₆) δ (ppm): 27.63. ¹³C-NMR (DMSO-*D*₆) δ (ppm): 36.4, 72.5 (d, *J* = 86.9 Hz), 119.1, 120.1, 124.7 (d, *J* = 5 Hz), 125.3, 126.5 (d, *J* = 5 Hz), 126.8, 126.9, 128.2 (d, *J* = 11.3 Hz), 128.4 (d, *J* = 10.1 Hz), 130.9, 131.4, 131.5, 131.7, 131.8, 133.0 (d, *J* = 92.0 Hz), 137.0, 140.5, 141.0, 142.2, 143.2. HRMS: *m/z* calcd for C₂₆H₂₁O₂P (M + H⁺): 396.4175, found: 396.1279.

Step 2 (method B): The alcohol obtained in step 1 (0.126 mmol, 0.050 g, 1 equiv.), was dissolved in DCM (0.4 mL) in a 5 mL round bottom flask and DMP (0.190 mmol, 0.0805 g, 1.5 equiv.) was added in three portions. The reaction medium was stirred in the dark for 2 h. The reaction mixture was then quenched with 2 mL of Na₂SO₃. The resulting mixture was extracted with 15 mL of DCM, then the combined organic layers were washed with 15 mL of saturated aqueous Na₂SO₃ and 15 mL of saturated aqueous NaHCO₃. After extraction, the organic layer was dried over MgSO₄ then, the solvent was removed under reduced pressure. The crude reaction mixture was then dried under vacuum for 2 h. A yellow solid was obtained (0.0426 g, 86% isolated yield). ¹H-NMR (CDCl₃) δ (ppm): 8.79 (s, 1H), 8.60–8.58 (d, *J* = 10 Hz, 1H), 7.93–7.86 (m, 6H), 7.60–7.56 (m, 3H), 7.53–7.49 (m, 4H), 7.44–7.39 (m, 2H), 3.97 (s, 2H). ³¹P-NMR (CDCl₃) δ (ppm): 22.77. ¹³C-NMR (CDCl₃) δ (ppm): 36.7, 120.0, 121.1, 125.1, 126.8 (d, *J* = 15.1 Hz), 128.3, 128.5, 129.5, 130.0 (d, *J* = 98.2 Hz), 131.6 (d, *J* = 8.8 Hz), 132.1 (d, *J* = 2.5 Hz), 135.1, 135.5, 139.9, 143.2, 144.85, 149.1, 203.4 (d, *J* = 80.6 Hz). HRMS: *m/z* calcd for C₂₆H₁₉O₂P (M + Na): 394.4016, found: 394.1123.

4.6 | Other chemicals

Cyclic trimethylpropane formal acrylate (CTFA) and the Flexibloc were supplied by Arkema. The Flexibloc is used in order to control the viscosity of the formulation. BAPO was purchased from Lambson. Dichloromethane (DCM) and acetonitrile were purchased from Carlo Ebra.

4.7 | UV-vis spectroscopy

UV-visible spectra were recorded in acetonitrile in a 1 cm square quartz cell by a JASCO V-730 spectrophotometer.

4.8 | RT-FTIR spectroscopy

A Jasco V-4100 Real Time Fourier transform infra-red spectrometer was used to follow the C=C double bond conversion versus time for the polymerization of 2 mm thick samples. All photopolymerizations were carried out under air at room temperature. A 405 nm LED with an irradiance of 170 mW/cm² was used to initiate the photopolymerization. The follow of the conversion was done by looking at the intensity decrease of the peak between 6100 and 6250 cm⁻¹ which corresponds to the C=C double bond of the acrylate function for thick samples.

4.9 | In vitro cytotoxicity of the ADPO-1

The cytotoxicity of the synthesized photoinitiator was evaluated in human umbilical vein endothelial cells (HUVECs) and human normal hepatocytes (L02) using MTT (3-(4,5-dimethylthiazol-2-yl)-2,5-diphenyltetrazole bromide) assay. Briefly, HUVECs were seeded onto 96-well plates at a density of 8 × 10³–1 × 10⁴ cells/well and incubated at 37°C and 5% CO₂ for 24 h. Meanwhile, a 100 mM stock solution of TPO and ADPO-1 was prepared in ethanol, which was then diluted to varying concentrations using DMEM (Dulbecco's Modified Eagle Medium) /F12—containing 10% FBS. After 24, 48, and 72 h of incubation with the cells, the media containing either TPO or ADPO-1 were removed and subsequently replaced with serum-free culture media. Finally, the cell viability was determined using MTT assay.

4.10 | 3D printings experiments

The 3D printing tests were carried out with an Anycubic Photon S 3D printer. The technology used is LCD screen Shadow Masking. The irradiation wavelength is 405 nm, and the irradiance is 0.81 mW/cm². The printed models were obtained from the website: thingiverse. To be printed, the .stl files were opened in the photon workshop software where the z lift speed of the platform was chosen at 3 mm/s, the z retract speed was chosen at 3 mm/s and the z lift distance was fixed at 6 mm. The thickness of each layer was fixed at 200 μm.

Subsequently, the different printing parameters, such as the irradiation time per layer, the irradiation time of the first layers, the number of first layers were defined according to the resin used. Finally the file was sliced and exported in .pws to be read by the 3D printer. The .pws file was copied to a USB key and opened with the Anycubic Photon S 3D printer. Once the 3D printing was completed, the resulting object was washed with ethanol and then post-cured under LED irradiation at 405 nm for 15 min.

Typically, resins used in 3D printing contained 10 wt % of Flexibloc, 89 wt% of CTFA monomer, and 1 wt% of photoinitiator.

AUTHOR CONTRIBUTIONS

Jacques Lalevee: Conceptualization (equal); formal analysis (equal); funding acquisition (equal); investigation (equal); methodology (equal); project administration (equal); resources (equal); supervision (equal); validation (equal); writing – review and editing (equal). **Loïc BUCHON:** Data curation (lead); writing – original draft (lead). **Jean-Michel BECHT:** Conceptualization (equal); formal analysis (equal); investigation (equal); methodology (equal); project administration (equal); resources (equal); supervision (equal); writing – review and editing (equal). **Laurent RUBATAT:** Conceptualization (equal); funding acquisition (equal); project administration (equal); writing – review and editing (equal). **Wei Wang:** Conceptualization (equal); data curation (equal); writing – review and editing (equal). **Hua Wei:** Conceptualization (equal); data curation (equal); writing – review and editing (equal). **Pu Xiao:** Conceptualization (equal); formal analysis (equal); investigation (equal); methodology (equal); writing – review and editing (equal).

ACKNOWLEDGMENTS

The Agence Nationale de la Recherche for the funding of this work: ANR-19-CE06-0017 (Project PIMS-3D).

DATA AVAILABILITY STATEMENT

The data that support the findings of this study are available from the corresponding author upon reasonable request.

ORCID

Jacques Lalevee  <https://orcid.org/0000-0001-9297-0335>

REFERENCES

- [1] T. D. Ngo, A. Kashani, G. Imbalzano, K. T. Q. Nguyen, D. Hui, *Compos. Part B Eng.* **2018**, *143*, 172.
- [2] S. C. Ligon, R. Liska, J. Stampfl, M. Gurr, R. Mülhaupt, *Chem. Rev.* **2017**, *117*, 10212.
- [3] A. Bagheri, J. Jin, *ACS Appl. Polym. Mater.* **2019**, *1*, 593.
- [4] J. Zhang, P. Xiao, *Polym. Chem.* **2018**, *9*, 1530.
- [5] M. Layani, X. Wang, S. Magdassi, *Adv. Mater.* **2018**, *30*, 1706344.
- [6] Z. Dong, H. Cui, H. Zhang, F. Wang, X. Zhan, F. Mayer, B. Nestler, M. Wegener, P. A. Levkin, *Nat. Commun.* **2021**, *12*, 247.
- [7] M. Manoj Prabhakar, A. K. Saravanan, A. Haiter Lenin, I. Jerin leno, K. Mayandi, P. Sethu Ramalingam, *Mater. Today Proc.* **2021**, *45*, 6108.
- [8] A. Medellin, W. Du, G. Miao, J. Zou, Z. Pei, C. Ma, *J. Micro Nano-Manuf.* **2019**, *7*, 31006.
- [9] M. Pagac, J. Hajnys, Q.-P. Ma, L. Jancar, J. Jansa, P. Stefek, J. Mesicek, *Polymer* **2021**, *13*, 598.
- [10] H. Quan, T. Zhang, H. Xu, S. Luo, J. Nie, X. Zhu, *Bioact. Mater.* **2020**, *5*, 110.
- [11] D. Ahn, L. M. Stevens, K. Zhou, Z. A. Page, *ACS Cent. Sci.* **2020**, *6*, 1555.
- [12] J. P. Fouassier, J. Lalevée, *Photoinitiators for Polymer Synthesis: Scope, Reactivity and Efficiency*, Wiley-VCH Verlag GmbH & Co. KGaA, Weinheim, Germany **2012**. <https://doi.org/10.1002/9783527648245>
- [13] P. Xiao, J. Zhang, F. Dumur, M. A. Tehfe, F. Morlet-Savary, B. Graff, D. Gimes, J. P. Fouassier, J. Lalevée, *Prog. Polym. Sci.* **2015**, *41*, 32.
- [14] C. Dietlin, S. Schweizer, P. Xiao, J. Zhang, F. Morlet-Savary, B. Graff, J.-P. Fouassier, J. Lalevée, *Polym. Chem.* **2015**, *6*, 3895.
- [15] Y. Zhang, Y. Xu, A. Simon-Masseron, J. Lalevée, *Chem. Soc. Rev.* **2021**, *50*, 3824.
- [16] H. Moseley, *Phys. Med. Biol.* **1994**, *39*, 1765.
- [17] S. M. Müller, S. Schlögl, T. Wiesner, M. Haas, T. Griesser, *ChemPhotoChem* **2022**, *6*, e202200091.
- [18] J. Lalevée, J.-P. Fouassier Eds., *Dyes and Chromophores in Polymer Science: Lalevée/Dyes and Chromophores in Polymer Science*, John Wiley & Sons, Inc., Hoboken, NJ, USA **2015**. <https://doi.org/10.1002/9781119006671>
- [19] A. Assmann, A. Vegh, M. Ghasemi-Rad, S. Bagherifard, G. Cheng, E. S. Sani, G. U. Ruiz-Esparza, I. Noshadi, A. D. Lassaletta, S. Gangadharan, A. Tamayol, A. Khademhosseini, N. Annabi, *Biomaterials* **2017**, *140*, 115.
- [20] E. A. Kamoun, A. Winkel, M. Eisenburger, H. Menzel, *Arab. J. Chem.* **2016**, *9*, 745.
- [21] Y. Bao, *Macromol. Rapid Commun.* **2022**, *43*, 2200202.
- [22] T. Sumiyoshi, W. Schnabel, *Makromol. Chem.* **1985**, *186*, 1811.
- [23] C. Dietlin, T. T. Trinh, S. Schweizer, B. Graff, F. Morlet-Savary, P.-A. Noiro, J. Lalevée, *Macromolecules* **2019**, *52*, 7886.
- [24] Y. Wu, R. Li, J. Ke, X. Cheng, R. Tang, Y. Situ, H. Huang, *Eur. Polym. J.* **2022**, *168*, 111093.
- [25] C. Dietlin, T. T. Trinh, S. Schweizer, B. Graff, F. Morlet-Savary, P.-A. Noiro, J. Lalevée, *Molecules* **2020**, *25*, 1671.
- [26] J. Wang, S. Stanic, A. A. Altun, M. Schwentenwein, K. Dietliker, L. Jin, J. Stampfl, S. Baudis, R. Liska, H. Grützmaker, *Chem. Commun.* **2018**, *54*, 920.
- [27] A. Eibel, M. Schmallegger, M. Zalibera, A. Huber, Y. Bürkl, H. Grützmaker, G. Gescheidt, *Eur. J. Inorg. Chem.* **2017**, *2017*, 2469.
- [28] H. Cai, S. Ji, J. Zhang, G. Tao, C. Peng, R. Hou, L. Zhang, Y. Sun, X. Wan, *Food Addit. Contam. Part A* **2017**, *34*, 1632.

- [29] B. Zeng, Z. Cai, J. Lalevée, Q. Yang, H. Lai, P. Xiao, J. Liu, F. Xing, *Toxicol. In Vitro* **2021**, *72*, 105103.
- [30] Y. Wu, J. Ke, C. Dai, J. Wang, C. Huang, Y. Situ, H. Huang, *Eur. Polym. J.* **2022**, *175*, 111380.
- [31] Y. Wu, R. Li, C. Huang, J. Wu, X. Sun, Y. Situ, H. Huang, *Prog. Org. Coat.* **2022**, *168*, 106876.
- [32] Y. Liu, T. Wang, C. Xie, X. Tian, L. Song, L. Liu, Z. Wang, Q. Yu, *Prog. Org. Coat.* **2020**, *142*, 105603.
- [33] <https://e-brochure.arkema.com/unlocking-the-next-revolution-product-sheet-3/article/1/>
- [34] B. Zhang, J. He, Y. Li, T. Song, Y. Fang, C. Li, *J. Am. Chem. Soc.* **2021**, *143*, 4955.

SUPPORTING INFORMATION

Additional supporting information can be found online in the Supporting Information section at the end of this article.

How to cite this article: L. Buchon, J.-M. Becht, L. Rubatat, W. Wang, H. Wei, P. Xiao, J. Lalevee, J. *Appl. Polym. Sci.* **2023**, e54694. <https://doi.org/10.1002/app.54694>